

From Noisy News Sentiment Scores to Interpretable Temporal Dynamics: A Bayesian State-Space Model

Ian Carbó Casals

January 23, 2026

Abstract

Text-based sentiment indicators are widely used to monitor public and market mood, but weekly sentiment series are noisy by construction. A main reason is that the amount of relevant news changes over time and across categories. As a result, some weekly averages are based on many articles, while others rely on only a few. Existing approaches do not explicitly account for changes in data availability when measuring uncertainty. We present a Bayesian state-space framework that turns aggregated news sentiment into a smoothed time series with uncertainty. The model treats each weekly sentiment value as a noisy measurement of an underlying sentiment process, with observation uncertainty scaled by the effective information weight n_{tj} : when coverage is high, latent sentiment is anchored more strongly to the observed aggregate; when coverage is low, inference relies more on the latent dynamics and uncertainty increases. Using news data grouped into multiple categories, we find broadly similar latent dynamics across categories, while larger differences appear in observation noise. The framework is designed for descriptive monitoring and can be extended to other text sources where information availability varies over time.

Keywords: Bayesian state-space models, sentiment analysis, news sentiment monitoring, news analytics, measurement error, time series smoothing, uncertainty quantification, hierarchical Bayesian modeling, natural language processing.

1. Introduction

Financial markets react quickly to new information. Because of this, many studies use sentiment from text (news, social media, or messaging apps) to understand investor mood, market risk, and possible price movements. Today, modern Natural Language Processing (NLP) models can score each message as positive or negative and can also classify messages into categories [Araci, 2019, Yin et al., 2019, Lewis et al., 2019]. However, when we aggregate these AI scores over time, the resulting sentiment series is often very noisy [Shapiro et al., 2022]. It can change a lot from week to week, not only because sentiment really changes, but also because the amount of available information changes. For example, a weekly sentiment value based on hundreds of messages is much more reliable than a value based on only a few messages.

This problem is naturally framed as a latent-state estimation problem: we observe noisy sentiment measurements, while the “true” sentiment is a hidden process that evolves over time. A classic solution for this type of problem is the Kalman Filter [Kalman, 1960], which estimates a hidden state using a transition model (how the state changes) and a measurement model (how observations are created). Later work extends this idea to settings where observation noise is unknown or changes over time, for example with variational Bayesian adaptive Kalman filters, which estimate both the hidden state and time-varying noise parameters [Huang et al., 2018]. In finance, similar dynamic models have been used for sentiment series, treating sentiment indices as noisy measurements of an underlying latent sentiment process and using filtering to separate long-term trends from short-term shocks [Vassallo, 2021]. More recently, hybrid methods combine large language models with Bayesian state-space models to improve forecasting by using semantic information from text [Cho et al., 2025].

Even with these advances, an important gap remains for sentiment built from irregular information streams, such as messaging platforms, social media, or news feeds. In these sources, the number of relevant messages can change strongly over time. Many existing models either assume a more stable flow of information or try to learn time-varying noise in a general way. But for sentiment data, the main driver of reliability is often simple and observable: how much evidence do we have. If we ignore this, we mix true sentiment changes with changes in data availability. This is especially important because recent research shows that using AI-generated variables as true data in econometric analysis can lead to biased estimates and invalid inference due to measurement error [Battaglia et al., 2024]. At the same time, recent surveys in financial AI emphasize that uncertainty quantification (both aleatoric and epistemic) is essential to make AI signals reliable for financial decision-making [Eggen et al., 2025]. Therefore, modeling measurement reliability is a first-order requirement for sentiment monitoring from text.

In this paper, we introduce a hierarchical Bayesian state-space model to build a stable and interpretable sentiment signal. We treat the observed weekly sentiment for each category as a noisy measurement of a latent sentiment state. The key idea is to scale observation noise using an information density term n_{tj} , defined as the total category-relevance weight in week t (a weighted volume rather than a raw message count). Unlike approaches that infer time-varying noise through generic latent volatility [Huang et al., 2018], we use an observable, data-driven reliability measure based on category relevance mass. When n_{tj} is high, the measurement is more precise and observation noise is smaller; when n_{tj} is low, uncertainty increases and the model relies more on latent temporal dynamics. A Bayesian formulation provides full posterior distributions for latent states and parameters, allowing us to report credible intervals and quantify uncertainty in a principled way. This is essential for monitoring noisy sentiment signals. Our approach follows the same filtering principle as adaptive Kalman filtering [Huang et al., 2018] and sentiment filtering in finance [Vassallo, 2021], but it provides a more direct and interpretable way to model changing measurement reliability in irregular news streams.

Our contributions are threefold. First, we introduce a Bayesian state-space model for category-level sentiment monitoring in which observation noise is scaled by information density, linking data availability to measurement uncertainty. Second, we use a hierarchical structure to share information across categories, improving robustness when some categories have few messages. Third, we provide an uncertainty-aware framework for monitoring sentiment dynamics, which can support more reliable downstream analysis and decision-making.

2. Methods

2.1 Data and Temporal Aggregation

2.1.1 News Collection and NLP Scoring

News articles were collected automatically from multiple public sources using a custom Python pipeline. The data were stored in a relational database and processed using pretrained natural language processing (NLP) models to obtain sentiment and category relevance scores for each article. The code used for data collection and NLP scoring, as well as the analysis scripts, is publicly available (see Section 6 for data and code availability).

Let X denote the text of a news article.

Sentiment. We use the FinBERT model to estimate the sentiment of each article [Araci, 2019]. For a given text X_i , the model outputs probabilities associated with positive, neutral, and negative sentiment:

$$POS(X_i), NEU(X_i), NEG(X_i) \in (0, 1)$$

with $POS(X_i) + NEU(X_i) + NEG(X_i) \approx 1$. We summarize these outputs into a single sentiment score defined as:

$$S(X_i) = POS(X_i) - NEG(X_i)$$

which takes values in the interval $[-1, 1]$. Positive values indicate predominantly positive sentiment, while negative values indicate predominantly negative sentiment.

Category Tagging. To assign news articles to thematic categories, we use the zero-shot classification model bart-large-mnli [Lewis et al., 2019, Yin et al., 2019]. Given a predefined set of m categories, the model returns a relevance score for each category. For a given article i with text X_i , we denote by:

$$C_{ij}(X_i) \in (0, 1) \quad j = 1, \dots, m$$

the relevance score of category j . For simplicity, we write C_{ij} for $C_{ij}(X_i)$ in the remainder of the paper. These scores are interpreted as soft weights, allowing a single article to contribute to multiple categories with different intensities.

2.1.2 Construction of Sentiment Scores

Each article is assigned to a unique time window according to its publication date. Time is divided into fixed windows of length Δt . In this study, we use weekly windows and set $\Delta t = 7$ days. Weekly windows are indexed as $t = 1, \dots, N$, from the week starting 2023-12-31 to the week starting 2025-11-30.

At the article level, the observed quantities are the sentiment scores S_i and the category relevance scores C_{ij} . In order to reduce noise in the category assignments, we apply a threshold to the relevance scores. Specifically, values below 0.25 are considered non-informative and are set to zero:

$$C_{ij} = 0 \quad \text{if } C_{ij} < 0.25$$

After thresholding, articles with null vectors were excluded from the analysis.

Using the processed category scores, we define the aggregated sentiment score for time window t and category j as a weighted average over all articles published in that interval. Let news_t denote the set of articles published in time window t . The aggregated sentiment is defined as:

$$y_{tj} = \frac{\sum_{i \in \text{news}_t} C_{ij} S_i}{\sum_{i \in \text{news}_t} C_{ij}}$$

Finally, categories for which no articles remain after this procedure in a large number of time windows are excluded from the analysis. Starting from an initial set of eight categories, this filtering step results in a final set of six categories used in the empirical analysis, which are shown in Figure 1.

2.1.3 Exploratory Analysis

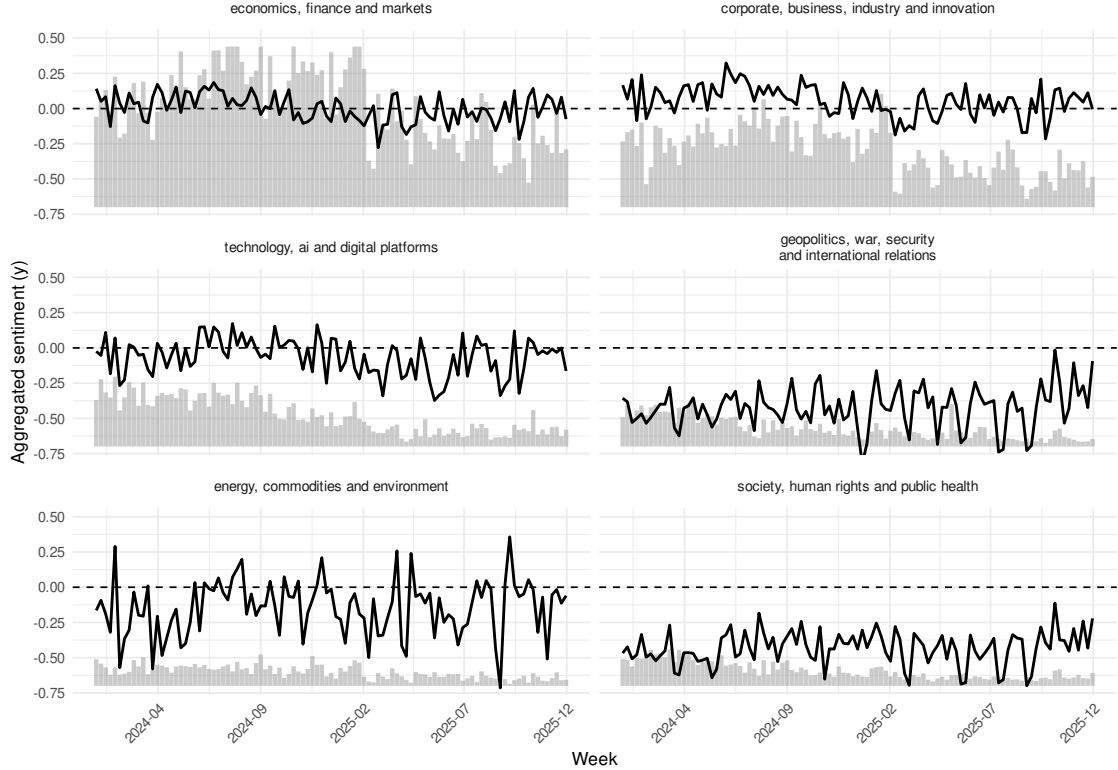


Figure 1: Aggregated sentiment y_{tj} (line) and effective weight n_{tj} (bars, globally rescaled) for each category.

Figure 1 shows the aggregated sentiment y_{tj} for each category together with the effective weight n_{tj} , defined as the total category relevance mass within each time window (see Section 2.2.2 for the formal definition). The bars represent n_{tj} and are globally rescaled for visual comparison. After preprocessing, no time windows with zero effective weight were observed in the 6 selected categories.

The dataset contains a total of 9,918 news articles with positive relevance for at least one category, corresponding to an average of approximately 99 articles per week. Data availability varies over time and, more clearly, across categories. Some categories are consistently supported by a larger amount of category-related news, while others exhibit much lower effective weights in many time windows.

This imbalance across categories motivates partial pooling and a state-space model in which observation uncertainty is allowed to vary with information density n_{tj} .

2.2 Bayesian State-Space Model for News Sentiment

We model the observed aggregated sentiment y_{tj} as a noisy measurement of an unobserved (latent) sentiment process x_{tj} evolving over time [Gelman et al., 2013, Durbin and Koopman, 2012].

2.2.1 Latent Sentiment Dynamics

For each category j , the latent sentiment is modeled as an autoregressive process of order one $AR(1)$ around a long-run mean μ_j :

$$\begin{aligned} x_{1j} &\sim \text{Normal}(\mu_j, \sigma_{\eta j}^2) \\ x_{tj} &\sim \text{Normal}\left((1 - \theta_j)\mu_j + \theta_j x_{t-1,j}, \sigma_{\eta j}^2\right) \quad t = 2, \dots, N \end{aligned}$$

The persistence parameter $\theta_j \in [0, 1]$ controls how strongly the current latent sentiment depends on the previous state. Values close to 1 imply high persistence (slow changes), while values closer to 0 imply faster mean reversion toward μ_j . The parameter $\sigma_{\eta j}$ controls the latent process variability.

2.2.2 Observation Model and Effective Weight

The observed aggregated sentiment y_{tj} is modeled as a noisy observation of x_{tj} :

$$y_{tj} \sim \text{Normal}(x_{tj}, \sigma_j^2/n_{tj})$$

We define x_{tj} as the latent state. Importantly, it represents the underlying mean of the observed sentiment process (what we would measure with complete coverage), not a different target outside this measurement process (e.g., the sentiment value that would be obtained if we had access to all relevant articles for category j in week t and measured them without error).

We adopt a Gaussian observation model. Although sentiment is bounded in $[-1, 1]$, the posterior predictive probability of generating values for y_{tj} outside $[-1, 1]$ is negligible (see Appendix A.2, Table 2; $\max_{tj} P(\text{out}) < 1.5 \times 10^{-3}$).

Here σ_j is the observation noise scale for category j . The term n_{tj} represents the effective amount of category-related information available in time window t for category j , defined as:

$$n_{tj} = \sum_{i \in \text{news}_t} C_{ij}$$

Intuitively, n_{tj} increases when more articles in window t are strongly related to category j (high C_{ij}). The scaling σ_j^2/n_{tj} is motivated by the fact that y_{tj} is a weighted average of many article-level sentiment scores. Under the assumption that these articles provide roughly independent and diverse evidence about category j in week t , weighted averages become more stable when they are computed from more effective evidence. For this reason, we model measurement uncertainty as decreasing with n_{tj} : when n_{tj} is large, y_{tj} is a more precise measurement of x_{tj} ; when n_{tj} is small, the model downweights y_{tj} and relies more on the latent dynamics.

2.2.3 Priors and Hierarchical Structure

The long-run mean μ_j is constrained to $[-1, 1]$ using a transformation:

$$\mu_j^{aux} \sim \text{Beta}(1, 1), \quad \mu_j = 2\mu_j^{aux} - 1$$

To share information across categories while allowing category-specific behavior, we place hierarchical priors on the persistence and noise parameters.

Persistence. We model θ_j on the logit scale:

$$\theta_j^{aux} \sim \text{Normal}(\mu_\theta, \sigma_\theta^2), \quad \theta_j = \frac{1}{1 + e^{-\theta_j^{aux}}}$$

with hyperpriors $\mu_\theta \sim \text{Normal}(0, 1^2)$ and $\sigma_\theta \sim \text{Lognormal}(\log(0.7), 0.35^2)$.

Noise scales. We model standard deviations on the log scale:

$$\begin{aligned} \log(\sigma_j) &\sim \text{Normal}\left(\mu_{\log(\sigma)}, \sigma_{\log(\sigma)}^2\right), \quad \sigma_j = e^{\log(\sigma_j)} \\ \log(\sigma_{\eta j}) &\sim \text{Normal}\left(\mu_{\log(\sigma_\eta)}, \sigma_{\log(\sigma_\eta)}^2\right), \quad \sigma_{\eta j} = e^{\log(\sigma_{\eta j})} \end{aligned}$$

The hyperpriors assigned are:

$$\begin{aligned} \mu_{\log(\sigma)} &\sim \text{Normal}(\log(0.15), 1^2), \quad \sigma_{\log(\sigma)} \sim \text{Lognormal}(\log(0.5), 0.35^2) \\ \mu_{\log(\sigma_\eta)} &\sim \text{Normal}(\log(0.05), 1^2), \quad \sigma_{\log(\sigma_\eta)} \sim \text{Lognormal}(\log(0.5), 0.35^2) \end{aligned}$$

This parameterization improves numerical stability in MCMC sampling and guarantees positivity of $\sigma_{\eta j}$ and σ_j .

3. Results

3.1 Posterior Inference on Model Parameters

We analyze the posterior distributions of the main model parameters and how they differ across categories. We focus on the persistence parameter θ_j , the latent process scale $\sigma_{\eta j}$, and the observation noise scale σ_j .

The results shown in this section are based on two estimations of the same state-space model fitted to the same data, with identical likelihood structure and priors. One estimation imposes full pooling across categories, while the other allows category-specific parameters through hierarchical priors.

In this section, black curves correspond to the pooled (simple) model, where a single parameter is shared across all categories. Colored curves correspond to the hierarchical model, where parameters are category-specific but partially pooled through hierarchical priors.

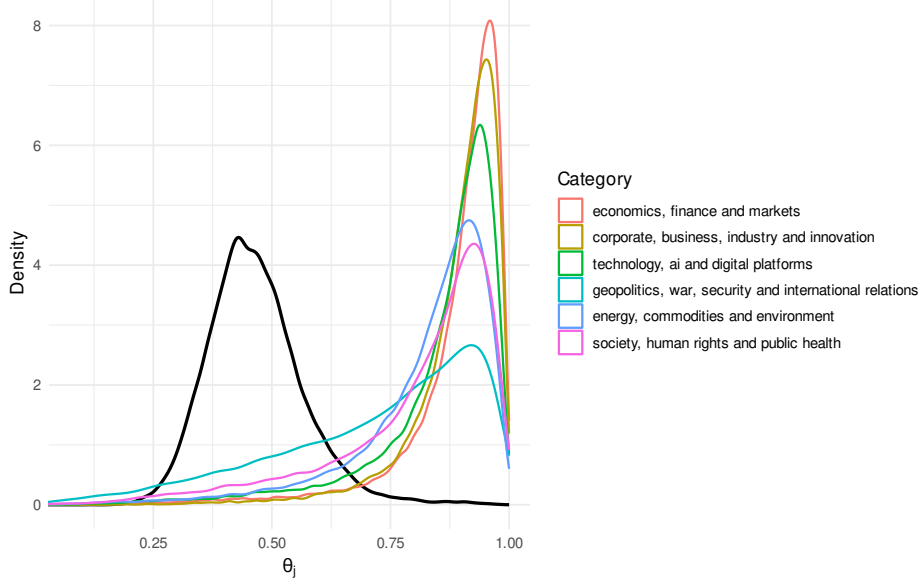


Figure 2: Posterior densities of the persistence parameter, pooled (black) vs category-specific (colors).

3.1.1 Persistence of sentiment dynamics

Figure 2 shows the posterior densities of the persistence parameter θ_j . Compared to the pooled model, the hierarchical model shows slightly different persistence levels across categories. However, these differences are relatively small, and the category-specific posteriors remain close to each other and centered around a common value of θ . This indicates that most of the temporal persistence is shared across categories, and that the main benefit of the hierarchical model comes from modeling other sources of variation, rather than from differences in persistence.

While the estimated persistence differs between the pooled and hierarchical models, this does not indicate a contradiction. In the pooled specification, a single persistence parameter must absorb most of the temporal structure. In the hierarchical model, part of this structure is instead captured by category-specific innovation and noise terms. As a result, the persistence parameter mainly reflects a common temporal component shared across categories.

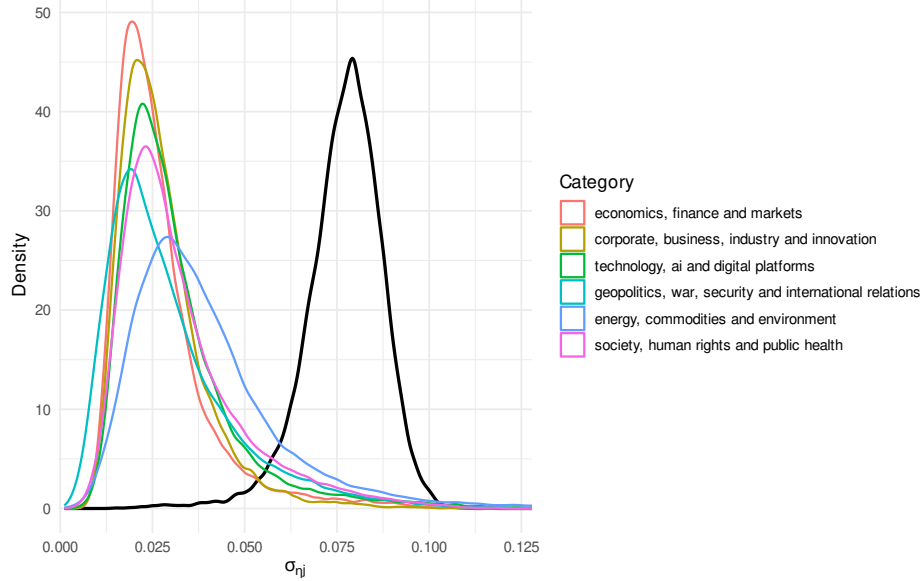


Figure 3: Posterior densities of the latent innovation parameter, pooled (black) vs category-specific (colors).

3.1.2 Latent innovation variability

Figure 3 presents the posterior densities of the latent innovation standard deviation σ_{η_j} , which controls short-term variability in the latent sentiment process x_{tj} .

The hierarchical model shows small differences across categories. Smaller values of σ_{η_j} correspond to smoother latent sentiment paths, while larger values allow for greater short-term variation. Overall, the innovation scale remains similar across categories, suggesting that short-term sentiment volatility is largely a shared feature rather than strongly category-specific.

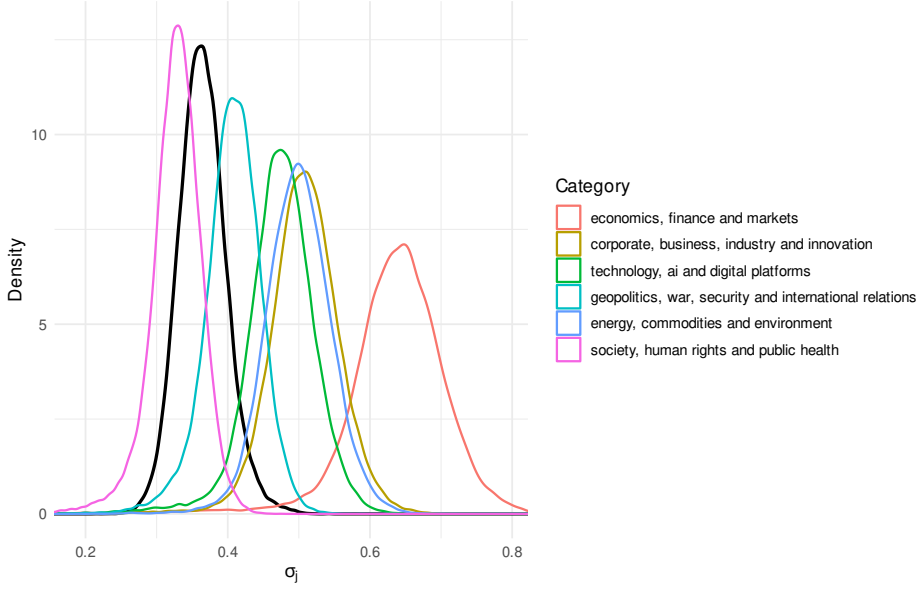


Figure 4: Posterior densities of the observation noise parameter, pooled (black) vs category-specific (colors).

3.1.3 Observation noise

Figure 4 shows the posterior densities of the observation noise parameter σ_j . This parameter measures how noisy the observed aggregated sentiment y_{tj} is around the latent sentiment x_{tj} , after accounting for the effective category weight n_{tj} .

We find that observation noise differs across categories. This means that the aggregated observed sentiment y_{tj} is a less precise measurement of the latent state for some categories than for others, likely reflecting differences in category ambiguity or variability in news content.

An additional comparison re-estimates the same model on the same data, allowing σ_j to vary by category while keeping θ and σ_η shared. In this setting, the posterior distributions of θ and σ_η closely match those obtained under the fully hierarchical model. This shows that the differences observed between the fully pooled and hierarchical models are driven primarily by allowing for heterogeneity in observation noise across categories, rather than by category-specific persistence or innovation dynamics.

3.2 Observed and Latent Sentiment

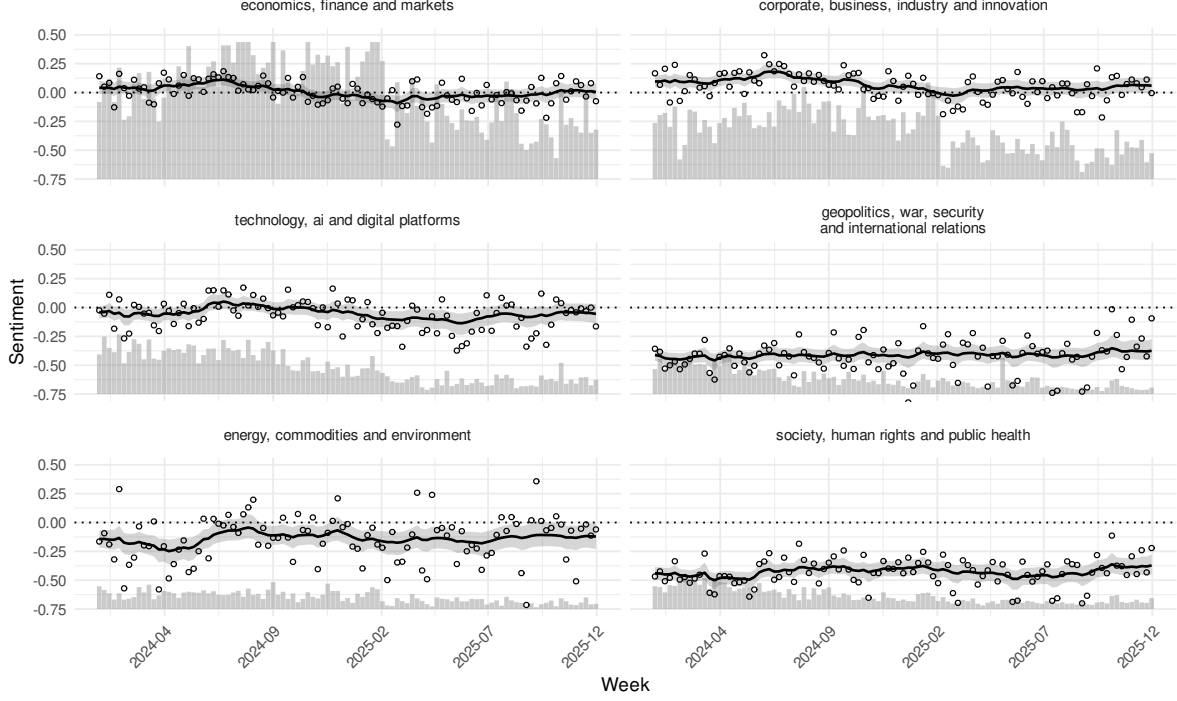


Figure 5: Observed y_{tj} (points) and latent state sentiment x_{tj} (solid line) with its 90% credible interval.

Figure 5 compares the observed aggregated sentiment y_{tj} (dots) with posterior estimates of the latent state x_{tj} across categories. The observed series y_{tj} can change quickly from week to week, while x_{tj} captures the more stable part of the sentiment dynamics over time.

The observed series y_{tj} itself can be viewed as a simple descriptive reference (direct aggregation) that does not model temporal dependence or uncertainty. In particular, short-term fluctuations in y_{tj} are more pronounced during periods of sparse coverage, making it difficult to assess whether changes reflect signal or measurement noise.

3.3 Model Comparison: Heteroscedastic versus homoscedastic observation noise

To isolate the role of information density in the observation model, we estimate two variants of the same state-space model on the same data, with identical priors and hierarchical structure, that differ only in the specification of the observation variance. This comparison provides a direct validation of the core modeling assumption: posterior uncertainty should increase mechanically as information density n_{tj} decreases. In the proposed heteroscedastic model:

$$y_{tj} \mid x_{tj} \sim N(x_{tj}, \sigma_j^2/n_{tj})$$

which can be written as $y_{tj} = x_{tj} + (\sigma_j/\sqrt{n_{tj}})\epsilon_{tj}$ with $\epsilon_{tj} \sim N(0, 1)$. This implies that lower n_{tj} should lead to higher measurement noise and wider posterior uncertainty about x_{tj} . In a homoscedastic variant, we keep all other components unchanged but use a constant observation variance:

$$y_{tj} \mid x_{tj} \sim N(x_{tj}, \sigma_j^2)$$

Because x_{tj} is latent, we do not test this scaling through direct residual standardization. Instead, we validate its observable consequence on posterior uncertainty. Let $Q_p(x_{tj})$ denote the posterior p-quantile of x_{tj} . We compute the 90% posterior interval width $w_{tj} = Q_{0.95}(x_{tj}) - Q_{0.05}(x_{tj})$ and regress it on $1/\sqrt{n_{tj}}$, including category fixed effects and an interaction with the homoscedastic variant. The regression output is reported in Appendix A.1. In the heteroscedastic specification, a one-unit increase in $1/\sqrt{n_{tj}}$ is associated with a 0.098 increase in w_{tj} , whereas in the homoscedastic variant the corresponding marginal effect is 0.041. The difference in slopes is statistically highly significant (interaction $p < 10^{-15}$), showing that the proposed scaling makes posterior uncertainty more responsive to changes in information density.

3.4 MCMC diagnostics

Posterior inference was performed using Markov Chain Monte Carlo methods implemented in JAGS [Plummer, 2003], accessed through the `r2jags` package in R.

We ran 3 MCMC chains of 255,000 iterations each, discarding the first 5,000 as burn-in and retaining every 25th draw, resulting in 10,000 posterior samples per chain (30,000 total). Convergence was assessed using the \hat{R} diagnostic and visual inspection of trace plots. For all main model parameters, \hat{R} values were close to 1, and trace plots showed stable mixing across chains. This suggests satisfactory convergence of the MCMC sampler. Representative trace plots for selected parameters and categories are reported in Appendix A.2, together with posterior predictive checks (PPC).

4. Discussion

Several limitations and modeling choices are worth noting. First, the category relevance threshold used to define the weights C_{ij} (0.25) is a pragmatic, dataset-specific choice. We selected it after manually inspecting a small sample of articles and their category scores, with the goal of cutting noise at a reasonable point for aggregation. This threshold is therefore somewhat arbitrary and could be tuned differently in other datasets; however, since it filters out low-confidence assignments, moderate changes around this value should have limited impact on the aggregated signals.

Second, the effective weight n_{tj} should be read as a simple and interpretable measure of how much relevant news evidence is available in each time window. In our setting, repeated coverage of the same story across outlets is not necessarily undesirable: if the same news appears multiple times, this may reflect that it is more important and more widely reported. Under the assumption that sources are sufficiently diverse, using n_{tj} as proposed provides a transparent way for the model to express higher uncertainty when coverage is sparse. Future work could make this step more explicit by measuring source diversity week by week.

Third, we model the latent dynamics as an $AR(1)$ process mainly for interpretability and parsimony. This provides a directly interpretable persistence parameter θ_j and keeps the model identifiable with limited time-series length per category. More flexible dynamics (e.g., higher-order autoregression) are possible, but would add complexity and reduce transparency, which is not the main goal in descriptive monitoring.

Finally, the sentiment and category scores depend on external NLP models (here, FinBERT and related components), which may be imperfect. A principled way to reduce reliance on a single model is to combine multiple model outputs through probabilistic fusion (e.g., [Amirzadeh et al., 2025]); however, due to limited resources we opted for a simpler pipeline to keep the example simple. As an additional robustness extension, one could replace Gaussian observation noise with a heavier-tailed alternative (e.g., Student- t), at the cost of extra parameters.

A natural extension of the framework is to account for systematic differences in news exposure. In this paper, sentiment is measured from the observed news flow, without modeling how different audiences may be exposed to different subsets of news. Future work could incorporate source-level or platform-level information to distinguish changes in measured sentiment from changes in the composition of the news flow (e.g., by weighting articles by source reach or accounting for differences in how news spreads across platforms).

More broadly, the framework is not limited to news. It applies whenever sentiment is derived from text and information availability changes over time. By producing smoothed trajectories with credible intervals that

reflect data availability, the model supports descriptive monitoring and quantitative comparisons across time and categories, including applications such as product reviews, brand tracking, and campaign monitoring.

5. Conclusions

This paper proposes a Bayesian state-space framework to analyze news-based sentiment dynamics across multiple thematic categories. Using aggregated sentiment scores extracted from news articles, the model separates short-term noise from smoother underlying sentiment trends by introducing a latent process that evolves over time. Unlike simple aggregation approaches, the proposed method provides a principled way to combine temporal smoothing with uncertainty quantification, while remaining closely linked to the observed data.

The empirical results indicate that persistence parameters θ_j and short-term variability are similar across categories, with only small differences between categories, while larger differences appear in the observation noise. The effective weight n_{tj} , which captures how informative the observed sentiment is in each time window, plays a key role in the model: when fewer relevant articles are available, posterior uncertainty increases and the latent state relies more strongly on temporal smoothing rather than on the observed data. This mechanism allows the model to adapt naturally to imbalances in data availability across time and categories.

Overall, the proposed framework is explicitly designed for descriptive monitoring of news sentiment, prioritizing interpretability and uncertainty quantification over forecasting accuracy, and it provides a stable representation of sentiment over time.

6. Data and Code Availability

To support reproducibility, the code used to collect and process the news data (Telegram ingestion, FinBERT sentiment scoring, BART-MNLI category relevance, and dataset export), as well as the analysis scripts for the Bayesian state-space model, is available at <https://github.com/Baileduke/bayesian-sentiment-state-space-model> [Carbó Casals, 2026]. This paper corresponds to the tagged GitHub release v1.0.0, which freezes the exact version of the code used to generate the results reported in this manuscript.

Appendix

A.1 Information-density calibration

This subsection reports the regression table for the validation described in Section 4.2.2. For each category j and time t , we compute the 90% posterior interval width of the latent state:

$$w_{tj} = Q_{0.95}(x_{tj}) - Q_{0.05}(x_{tj})$$

where $Q_p(x_{tj})$ denotes the posterior p-quantile of x_{tj} . We then estimate the following linear model:

$$w_{tj} = \beta_0 + \beta_1 \frac{1}{\sqrt{n_{tj}}} + \beta_2 I_{homo} + \beta_3 I_{homo} \frac{1}{\sqrt{n_{tj}}} + \gamma_j + \epsilon_{tj}$$

where $I_{homo} = 1$ for the Homoscedastic variant and $I_{homo} = 0$ for the Heteroscedastic model, and γ_j denotes category fixed effects.

Table 1: Linear model for the 90% posterior interval width $w_{tj} = Q_{0.95}(x_{tj}) - Q_{0.05}(x_{tj})$ as a function of $1/\sqrt{n_{tj}}$, with category fixed effects and an interaction with the homoscedastic variant.

Term	Estimate	Std. Error	t value	p value
(Intercept)	0.0927	0.0012	74.97	0e+00
1/sqrt(n_tj)	0.0978	0.0046	21.33	0e+00
I_homo	0.0080	0.0016	5.09	4e-07
I_homo × 1/sqrt(n_tj)	-0.0566	0.0053	-10.72	0e+00

Note: Category fixed effects are included but not shown for brevity. $N = 1212$, Adjusted $R^2 = 0.8126$.

A.2 Model diagnostics

Table 2 reports summary posterior predictive check (PPC) metrics for the aggregated sentiment series. The 80% and 95% predictive intervals cover the observed data at roughly the expected rates, although the 80% intervals are a bit too wide. The posterior predictive probability of generating values outside the valid sentiment range $[-1, 1]$ is negligible.

Table 2: Posterior predictive check (PPC) summary metrics for aggregated sentiment by category.

Category	Cov 80%	Cov 95%	p (mean)	P(out)
economics, finance and markets	0.871	0.99	0.554	0.000000
corporate, business, industry and innovation	0.881	0.98	0.790	0.000000
technology, ai and digital, platforms	0.832	1.00	0.826	0.000000
geopolitics, war, security and international, relations	0.851	0.98	0.706	0.000475
energy, commodities and environment	0.901	0.96	0.574	0.001430
society, human, rights and public, health	0.861	0.99	0.612	0.000099

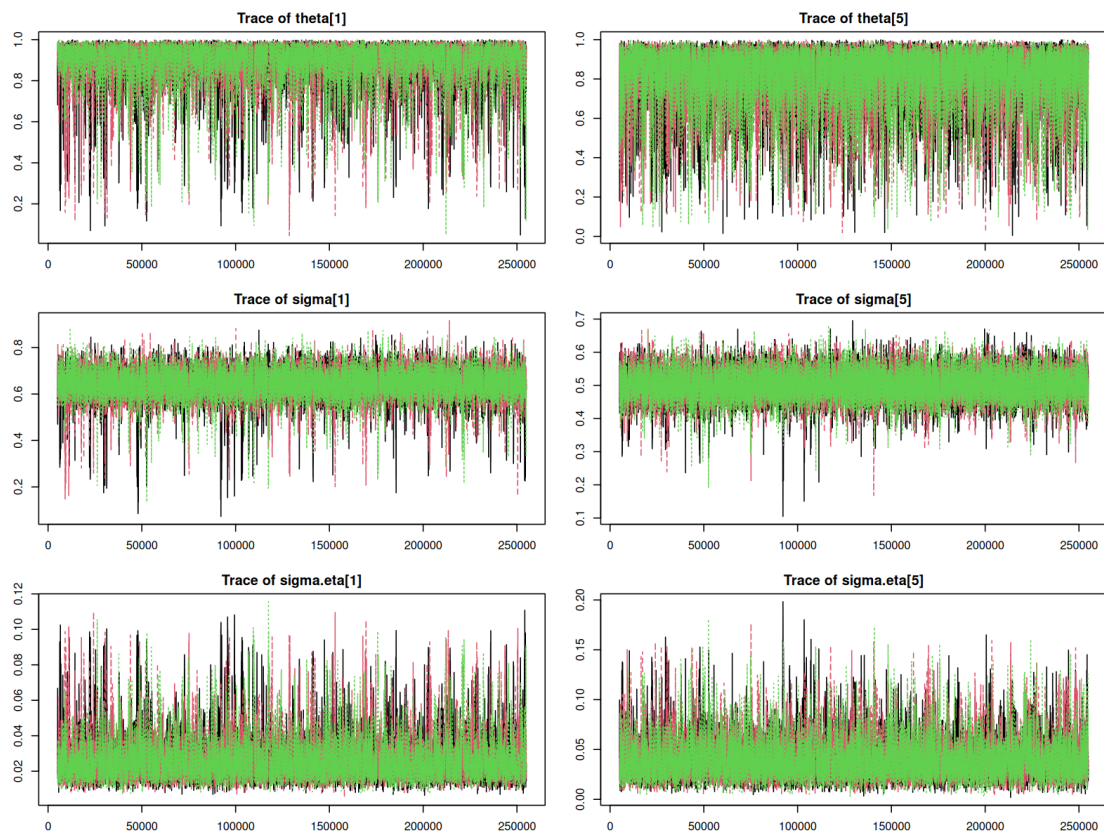


Figure 6: Trace plots for selected parameters in two representative categories (Economics, Finance and Markets; Energy, Commodities and Environment).

Acknowledgements

I am grateful to Jordi Villà i Freixa, Full Professor at UVic–UCC and group leader of the Computational Biochemistry and Biophysics Lab (CBBL) at IRIS-CC, for his guidance and constructive feedback throughout the development of this manuscript.

References

Rasoul Amirzadeh, Dhananjay Thiruvady, and Fatemeh Shiri. Bayesian network fusion of large language models for sentiment analysis, 2025. URL <https://arxiv.org/abs/2510.26484>.

Dogu Araci. Finbert: Financial sentiment analysis with pre-trained language models, 2019. URL <https://arxiv.org/abs/1908.10063>.

Laura Battaglia, Timothy Christensen, Stephen Hansen, and Szymon Sacher. Inference for regression with variables generated by ai or machine learning. Cowles Foundation Discussion Paper 2421, Cowles Foundation for Research in Economics, Yale University, 2024. URL <https://elischolar.library.yale.edu/cowles-discussion-paper-series/2831>.

Ian Carbó Casals. bayesian-sentiment-state-space-model (v1.0.0). <https://github.com/Baileduke/bayesian-sentiment-state-space-model>, 2026. GitHub repository, release v1.0.0.

Sungjun Cho, Changho Shin, Suenggwan Jo, Xinya Yan, Shourjo Aditya Chaudhuri, and Frederic Sala. Llm-integrated bayesian state space models for multimodal time-series forecasting, 2025. URL <https://arxiv.org/abs/2510.20952>.

James Durbin and Siem Jan Koopman. *Time Series Analysis by State Space Methods*. Oxford University Press, 2012.

Sivert Eggen, Tord Johan Espe, Kristoffer Grude, Morten Risstad, and Rickard Sandberg. Financial time series uncertainty: A review of probabilistic ai applications. *Journal of Economic Surveys*, 2025. URL <https://onlinelibrary.wiley.com/doi/abs/10.1111/joes.70018>.

Andrew Gelman et al. *Bayesian Data Analysis*. CRC Press, 2013.

Yulong Huang, Yonggang Zhang, Zhemin Wu, Ning Li, and Jonathon Chambers. A novel adaptive kalman filter with inaccurate process and measurement noise covariance matrices. *IEEE Transactions on Automatic Control*, 63(2):594–601, 2018. doi: 10.1109/TAC.2017.2730480. URL <https://ieeexplore.ieee.org/document/8025799>.

R. E. Kalman. A new approach to linear filtering and prediction problems. *Journal of Basic Engineering*, 82 (1):35–45, 1960. doi: 10.1115/1.3662552. URL <https://doi.org/10.1115/1.3662552>.

Mike Lewis, Yinhan Liu, Naman Goyal, Marjan Ghazvininejad, Abdelrahman Mohamed, Omer Levy, Ves Stoyanov, and Luke Zettlemoyer. Bart: Denoising sequence-to-sequence pre-training for natural language generation, translation, and comprehension, 2019. URL <https://arxiv.org/abs/1910.13461>.

Martyn Plummer. Jags: A program for analysis of bayesian graphical models using gibbs sampling. *Proceedings of the 3rd International Workshop on Distributed Statistical Computing*, 2003.

Adam Hale Shapiro, Moritz Sudhof, and Daniel J. Wilson. Measuring news sentiment. *Journal of Econometrics*, 228(2):221–243, 2022. ISSN 0304-4076. doi: <https://doi.org/10.1016/j.jeconom.2020.07.053>. URL <https://www.sciencedirect.com/science/article/pii/S0304407620303535>.

Davide Vassallo. *Dynamic models for financial and sentiment time series*. PhD thesis, Scuola Normale Superiore, Pisa, Italy, 2021. URL <https://hdl.handle.net/11384/109584>.

Wenpeng Yin, Jamaal Hay, and Dan Roth. Benchmarking zero-shot text classification: Datasets, evaluation and entailment approach, 2019. URL <https://arxiv.org/abs/1909.00161>.